JGR Atmospheres

RESEARCH ARTICLE
10.1029/2025JD045263

Special Collection:
Advances in Earth's Energy Balance, Aerosols, Cloud Processes & Climate

Constraining the Aerosol Effects on Deep Convective Clouds by Considering the Coupling Between Clouds and the Planetary Boundary Layer

Natalia Roldán-Henao[1], Zhanqing Li[1], Tianning Su[1,2], Jiwen Fan[3], and John Yorks[4]

[1]Department of Atmospheric and Oceanic Sciences and ESSIC, University of Maryland, College Park, MD, USA, [2]Lawrence Livermore National Laboratory, Livermore, CA, USA, [3]Argonne National Laboratory, Lemont, IL, USA, [4]NASA Goddard Space Flight Center, Greenbelt, MD, USA

Abstract Several mechanisms have been proposed for the aerosol invigoration effect. Although their principles are well established, their actual magnitudes and roles in cloud development remain uncertain and debatable. This uncertainty partly stems from observational-based studies, in which it has been challenging to separate the co-variability between aerosols and meteorology. Addressing this problem requires large data samples. To this end, this study employs the Atmospheric Radiation Measurement data set expanding to 16 years (some up to 17 years, compared to 10 years in previous work) in the U.S. Southern Great Plains. It also conducts a more careful and rigorous analysis to isolate the influences of convective available potential energy (CAPE) and synoptic patterns to address a previously raised concern. We incorporated a new key process affecting aerosol-cloud interaction: cloud-surface coupling. The state/degree of the coupling relationship turns out to play an important role in the invigoration effect. Our analysis reinforces earlier findings of a robust positive relationship between cloud thickness and aerosol loading across CAPE percentiles—but only under cloud-surface coupled conditions. The increase in cloud thickness with aerosol loading is most pronounced in coupled clouds with high CAPE and bases below 1 km. Coupled clouds with bases below 1 km thicken between 1 and 4 km, depending on the CAPE percentile. Decoupled clouds show no such systematic changes. Synoptic patterns also lead to different strengths of the invigoration effect. Clean and polluted air masses are predominantly associated with northerly and southerly winds, respectively, with a stronger invigoration effect in cleaner air masses.

Plain Language Summary Atmospheric aerosols are small particles essential for cloud formation, as they provide the surface for water vapor to condense and create cloud droplets in the atmosphere. Understanding these aerosol-cloud interactions is crucial for comprehending cloud properties and their evolution. However, studying these interactions is particularly challenging in deep convective clouds (DCCs), where complex physical processes occur. One hypothesis suggests that aerosols may intensify DCCs, a phenomenon known as the aerosol invigoration effect. This effect remains uncertain and debated, partly due to covariabilities between aerosols and meteorological factors such as Convective Available Potential Energy (CAPE). In this study, we evaluate the invigoration effect while introducing the concept of cloud-surface coupling, which assesses whether clouds interact with the underlying surface. In other words, we examine whether clouds are coupled or decoupled from the surface. Our observational framework investigates how cloud thickness responds to variations in aerosol concentration while constraining meteorological variations for both coupled and decoupled conditions. Positive relationships exist between cloud thickness and aerosol concentration for coupled clouds for different and narrow ranges of CAPE, but not for decoupled ones, reinforcing the aerosol invigorating effect. More studies are warranted concerning its general validity under different aerosol and meteorological conditions.

Key Points:

- Cloud-surface coupling is a determinant factor in the aerosol invigoration effect, while the convective available potential energy (CAPE) also plays an important role
- Positive relationships exist between cloud thickness and aerosol loading across different CAPE percentiles
- Distinct synoptic weather patterns lead to different strengths of the aerosol invigoration effect

Supporting Information:

Supporting Information may be found in the online version of this article.

Correspondence to:
Z. Li,
zhanqing@umd.edu

Citation:
Roldán-Henao, N., Li, Z., Su, T., Fan, J., & Yorks, J. (2026). Constraining the aerosol effects on deep convective clouds by considering the coupling between clouds and the planetary boundary layer. *Journal of Geophysical Research: Atmospheres*, *131*, e2025JD045263. https://doi.org/10.1029/2025JD045263

Received 26 AUG 2025
Accepted 1 APR 2026

Author Contributions:
Conceptualization: Natalia Roldán-Henao, Zhanqing Li, Tianning Su, Jiwen Fan, John Yorks
Data curation: Natalia Roldán-Henao, Tianning Su
Formal analysis: Natalia Roldán-Henao
Funding acquisition: Zhanqing Li, John Yorks
Investigation: Natalia Roldán-Henao
Methodology: Natalia Roldán-Henao, Zhanqing Li, Tianning Su

1. Introduction

Aerosols can act as Cloud Condensation Nuclei (CCN) under specific conditions, influencing both the macro- and microphysical properties of clouds. This interaction between aerosols and clouds depends on numerous factors such as the type of cloud, the prevailing meteorological conditions, and the characteristics of the aerosols. As a result, many aerosol-cloud interactions (ACIs) have been documented (e.g., Abbott & Cronin, 2021; Fan et al., 2016, 2018; Khain, 2009; Khain et al., 2008; Lebo & Morrison, 2014; Li et al., 2016, 2019; Liu et al., 2022; Stevens & Feingold, 2009; Tao et al., 2012).

Project administration: Zhanqing Li
Resources: Zhanqing Li, John Yorks
Software: Natalia Roldán-Henao
Supervision: Zhanqing Li
Validation: Natalia Roldán-Henao
Visualization: Natalia Roldán-Henao
Writing – original draft: Natalia Roldán-Henao
Writing – review & editing: Zhanqing Li, Tianning Su, Jiwen Fan, John Yorks

Among the various cloud types, the aerosol impact on deep convective clouds (DCCs) is especially complicated due to the intricate microphysics of multi-phase clouds, meteorological factors affecting DCCs, and a wide variety of aerosols that may serve as CCN and/or ice-nucleation (IN). All these factors make both observational and modeling investigations of ACI for DCC exceptionally challenging, as recently reviewed in Fan and Li (2022), Varble et al. (2023), and Fan et al. (2025). Additionally, uncertainties in cloud physics—particularly in ice-phase processes, collision and coalescence, and droplet breakup—hinder a comprehensive understanding of aerosol invigoration. As a result, studies have reported various outcomes, with some indicating enhanced convection or invigoration while others suggest no effect and enervation. Several mechanisms for aerosol convective invigoration have been proposed. The most well-known and the center of the debate are: (a) freezing-induced or cold-phase invigoration (Andreae et al., 2004; Rosenfeld et al., 2008); and (b) the condensational or warm-phase invigoration (Cotton & Walko, 2021; Fan et al., 2018). Both mechanisms are supported by theoretical inference and model calculations (Rosenfeld et al., 2008; Khain et al., 2008; Tao et al., 2012; Fan et al., 2012, 2018; Morrison & Grabowski, 2013; Cotton & Walko, 2021), and observational analyses (Andreae et al., 2004; Fan et al., 2025; Koren et al., 2014; Li et al., 2011; Yuan et al., 2011), while some studies refute them (Grabowski & Morrison, 2021; Igel & van den Heever, 2021; Varble, 2018; Öktem et al., 2023).

As noted in Varble et al. (2023) and Fan et al. (2025), the persistent lack of consensus regarding the invigoration effect stems largely from the inherent limitations of current observational data and analyses. Specifically, studying ACI for DCCs presents several key challenges, including: (a) the lack of measurements of crucial cloud microphysical, dynamical, and thermodynamical properties, which often forces studies to rely on indirect proxies, such as aerosol optical depth for CCN at the cloud base (Quaas et al., 2020); (b) The lack of coincidental measurements of aerosol, cloud, and meteorology in both time and space (Fan et al., 2025); (c) The often incomplete or insufficient duration of measurements that complicates any efforts to distinguish a true aerosol effect from the illusion of its co-variability, as indicated in Varble (2018; hereafter Varble18); and finally, (d) the fact that surface aerosol measurements made on the ground may not accurately reflect the aerosols supplied to updrafts that affect clouds (Fan et al., 2025). This problem can be greatly alleviated when clouds are coupled with the surface (Su et al., 2024).

These observational limitations, including the issues of sample size and meteorology co-variability, are exemplified by the results found for the U.S. Southern Great Plains (SGP). Employing 10 years of observational data from SGP, Li et al. (2011) analyzed the impact of aerosol on DCC and found that both cloud-top height and thickness increase with aerosol number concentration in DCCs with warm and low bases. In a revisit of this study, Varble18 argued first that the data samples were not sufficiently large to definitively link the observed increases in cloud-top height and thickness to aerosol loading. Second, they found a positive relationship between aerosol and the CAPE and thus argued that it could be the CAPE that ultimately drives the cloud development. Therefore, further investigations are essential to understand the impact of aerosols by better accounting for the influences of meteorological variables using a larger number of data samples.

In this investigation, we revisit Li et al. (2011) and conduct a more rigorous examination and address some of the limitations noted by Varble18 and Varble et al. (2023). Fan et al. (2025) addressed a couple of issues in these studies and found negligible co-variability when aerosols and CAPE were sampled from the clear-sky conditions prior to the presence of cloud objects. Note that once a cloud is well developed, the effect of ACI is already incorporated into cloud dynamics as mediated by CAPE. Moreover, an overlapping problem in the sampled DCC cloud objects (i.e., the beginning of a DCC was selected ahead of the ending of a previous DCC, resulting in duplication of cloud samples) was found in Varble18. When the overlapped DCCs in Varble18 were removed, a positive relationship between aerosol and CAPE no longer existed (Fan et al., 2025).

This investigation further addresses the limitations of the previous observational frameworks. Firstly, as noted by Varble et al. (2023), observational studies often rely on surface-based measurements of condensation nuclei (CN). These measurements require that convective clouds form within a certain range and direction for them to influence cloud inflow. Although obtaining direct measurements of aerosol concentration in the cloud inflow remains challenging, Su et al. (2024) found that incorporating cloud-surface or cloud-Planetary Boundary Layer (PBL) coupling in ACI studies improves the representation of aerosol concentration below cloud bases when using surface measurements, leading to improved estimation of the ACI. Therefore, this study explicitly incorporates cloud–surface coupling, thereby improving the representation of aerosols at the cloud base. Second, this investigation expands the analysis of Li et al. (2011) and Varble18 to cover at least 16 years, which helps

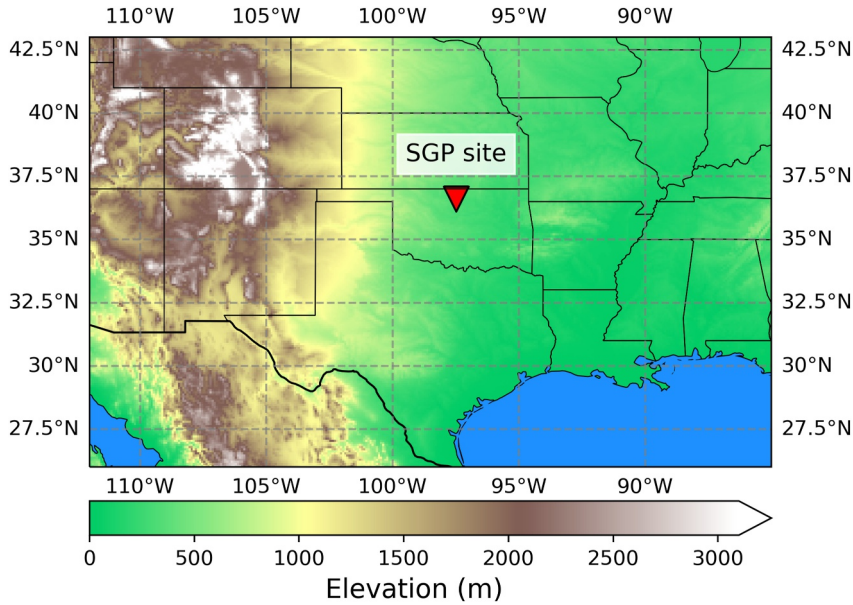

Figure 1. Geographical location of the Atmospheric Radiation Measurement U.S. Southern Great Plains site. Background colors correspond to surface elevation from the Altimeter Corrected Elevations, Version 2 (ACE2).

more robustly disentangle the roles of aerosols from meteorology. Finally, a key difference between this investigation and Li et al. (2011) is the inclusion and constraint of CAPE, the Level of Neutral Buoyancy (LNB), and the Level of Free Convection (LFC) in our analyses to help remove/suppress the influence of meteorological variability on convection. By constraining these variables, we aim to better isolate aerosol effects from meteorological confounders—an important methodological improvement relative to previous studies.

This paper is structured as follows: Section 2 describes the use of Atmospheric Radiation Measurement (ARM) data and our research method. Section 3 presents findings related to cloud-surface coupling and its influences on the ACI. This section conducts a sensitivity analysis of meteorological variables and evaluates the influences of numerous meteorological variables on–cloud, especially on the relationship between aerosol and cloud thickness, following the recommendations of Varble et al. (2023). Section 4 concludes the study and discusses its limitations.

2. Data and Methodology

2.1. Data

To investigate the aerosol effect on DCCs, we used data from the Department of Energy (DOE) ARM at the Central Facility in the U.S. Southern Great Plains in Oklahoma. Figure 1 shows the geographical location of SGP as well as the surface elevation. According to the ARM website (https://armgov.svcs.arm.gov/capabilities/observatories/sgp), SGP is located on 160 acres of cattle pasture and farm land dominated by wheat fields. On this site, the landscape and topography are relatively simple compared to those of complex terrain sites (Krishnamurthy et al., 2021). However, Oklahoma is characterized by greater topographic heterogeneity, with elevations ranging from 300 m to over 1,200 m above sea level in the northwest Panhandle (Brotzge & Richardson, 2003). The state's climate is influenced by different air masses, including warm, humid air from the Gulf of Mexico and cold, dry air from Canada. The land cover on larger scales is also diverse, with forests dominating the eastern one-third of the state, while the western one-half is primarily agricultural and grassland (Brotzge & Richardson, 2003).

As mentioned, this investigation uses multiple data sets from SGP. These data sets consist of simultaneous measurements that are averaged as 10-min means of aerosol, cloud, and meteorology. Our analyses involve the use of different variables whose periods of data availability differ somewhat. For those related to CAPE, they are for the period of 11/1998–06/2015 (~16 years) during which Mergesonde data were available. For other analyses without CAPE, they are for the period of 11/1998–07/2016 (~17 years), dictated by the availability of seamless

Table 1
List of the Variables and Products Used in This Investigation

Variable	Product	Instrument/Source	Period
Cloud boundaries (cloud-base and cloud-top heights)	CLDTYPE (DOI: 10.5439/1349884)	Micropulse Lidar, Ceilometer, and weather Radar	November 1998–July 2016
Aerosol Number Concentration	Aerosol Observing System (AOS) (DOI: 10.5439/1988399)	Condensation particle counter (CPC)	November 1998–July 2016
Rainfall	CLDTYPE	Micropulse Lidar, Ceilometer, and weather Radar	November 1998–July 2016
Cloud type	CLDTYPE	Micropulse Lidar, Ceilometer, and weather Radar	November 1998–July 2016
Planetary Boundary Layer Height	Retrievals based on the Different Thermo-Dynamic Stability (DTDS) algorithm by Su et al. (2020).	Micropulse Lidar	November 1998–July 2016
Temperature, relative humidity, wind direction, and atmospheric pressure profiles	Merged Sounding profiles derived with first and second Mace algorithms (MERGESONDE).	Merged sounding	November 1998–June 2015
Temperature and geopotential height at 850 hPa	ERA5	Hourly Reanalysis	November 1998–July 2016

aerosol data from the Aerosol Observing System. Similar to the approach taken by Li et al. (2011), we sampled aerosol and meteorological data at every time step within the cloud object, as the sensitive analysis of CAPE necessitates a larger number of samples. In addition, we use the ECMWF Reanalysis v5 (ERA5) reanalysis data at 850 hPa to investigate large-scale weather patterns across the continental U.S. Table 1 lists all the variables and products used in this investigation.

As noted from Table 1, this investigation relies on the ARM Value-Added Product (VAP) named CLDTYPE (DOI: 10.5439/1349884). CLDTYPE provides cloud boundaries (top and base) retrievals obtained from the Active Remote Sensing of Clouds (ARSCL) VAP (ARSCL, DOI: 10.5439/1996112) product. This product merges Micropulse LiDAR (MPL), Ceilometer, and a millimeter wavelength cloud radar (MMCR) information to produce a time series of the vertical distribution of clouds over the ARM sites following Clothiaux et al. (2000). Combining these three sensors helps to overcome the individual limitations of each and provides a more robust cloud detection product. The ARM MPL operates at 532 nm and has a temporal resolution of 10–30 s and a vertical resolution of 30 m. The Ceilometers operate at 910 nm and have a vertical resolution of 10 m and a temporal resolution of 2 s (Münkel et al., 2007). Finally, the MMCR operates at a frequency of 35 GHz with varying spatial/temporal resolution based on its operational mode.

To study aerosol impact on DCCs, we employ simultaneous measurements of cloud boundaries and geometrical thickness, aerosol number concentration, and Planetary Boundary Layer Height (PBLH). Our analysis considers only single-layer clouds with bases below 4 km. Using single-layer clouds prevents contamination from multiple cloud layers, and taking clouds with bases below 4 km constrains the cloud-surface coupling evaluation to only clouds that could be coupled to the surface when using the PBLH as the maximum height at which the surface fluxes reach. Additionally, since LiDARs encounter significant limitations in rainy conditions due to signal attenuation, we eliminated cases of immediate rain occurrence and rainfall events within an hour and a half prior. The cloud geometrical thickness was computed as the difference between the cloud base height (CBH) and the cloud top height (CTH).

2.2. Definition of Cloud-Surface Coupling and Its Determination

PBL processes are crucial in convective initiation and the formation of boundary-layer clouds (Berg & Stull, 2005; Betts, 2009; Golaz et al., 2002). A significant portion of clouds is influenced by surface fluxes transmitted through the PBL (Betts, 2009; Ek & Holtslag, 2004), particularly when a dynamically coupled cloud–surface system is established. While cloud–PBL interactions have been widely studied, the explicit role of

cloud–surface coupling in modulating ACI over land has only recently begun to receive attention (Su et al., 2024). In addition to the scarcity of ACI-related investigations involving cloud–surface coupling, the definition of coupling itself remains somewhat ambiguous. Earlier definitions were primarily derived from marine boundary layer studies, where a coupled state is typically characterized by well-mixed profiles of moisture conserved variables throughout the PBL (Bretherton & Wyant, 1997; Dong et al., 2015). However, this framework does not readily translate to land-based clouds, where more complex thermodynamic conditions lead to substantial vertical variability (Berg & Stull, 2005). As a result, both the definition and identification of coupling over land diverge from their marine counterparts.

Cloud–surface coupling describes whether turbulent fluxes originating at the land surface can reach and influence cloud properties. When clouds are dynamically connected to surface sources of heat, moisture, and aerosols, they are considered "coupled" (Dong et al., 2015; Hogan et al., 2009; Su et al., 2022; Zheng et al., 2018); if this connection is disrupted (e.g., due to a detached layer above the PBL), they are "decoupled." In other words, coupled clouds interact directly with surface forces, whereas decoupled clouds do not. The schematic and definition of the coupling was given in Su et al. (2022, 2024). Cloud-surface coupling is relevant in ACI investigations because different coupling regimes have distinct characteristics that affect ACIs, including the vertical distribution of aerosols beneath the cloud. For instance, in coupled regimes, aerosols are generally well mixed throughout the sub-cloud layer (i.e., inside the PBL), making aerosol measurements taken at ground level a good proxy for CCN at the cloud base. In contrast, decoupled clouds exhibit a more stratified distribution, with much higher aerosol loading near the surface than below the cloud base (Su et al., 2024), making the same aerosol measurements a bad proxy for CCN at the cloud base. These differences significantly affect our ability to quantify and evaluate the ACI.

A key parameter for diagnosing cloud–surface coupling is the PBLH, which marks the top of the turbulent mixing layer where surface-generated fluxes can influence cloud development. In this study, we determine coupling by comparing the PBLH with the CBH, following the LiDAR-based methodology developed by Su et al. (2022) and extended to multiple ARM sites in Roldán-Henao et al. (2024). Specifically, we classify a convective cloud as coupled if its CBH lies near or below the LiDAR-derived PBLH, indicating that the cloud is dynamically linked to surface heat, moisture, and aerosol sources. Conversely, clouds with bases significantly above the PBLH are classified as decoupled. PBLH estimates are derived from the Different Thermo-Dynamic Stability (DTDS) algorithm (Su et al., 2020), which improves upon traditional Micropulse LiDAR (MPL) retrievals by integrating backscatter gradients and thermodynamic constraints such as the lifted condensation level. This method has been validated across multiple ARM sites, showing good agreement with radiosonde-derived PBLH ($r > 0.77$), lending confidence to our classification. Details on the threshold criteria and validation for this methodology can be found in Su et al. (2022) and Roldán-Henao et al. (2026), including evaluations under diverse meteorological conditions.

The approach used here also accounts for the horizontal and vertical extents of clouds. We understand that coupling is not a fixed state, but a process that occurs throughout the entire cloud lifecycle. To address temporal variability and cloud evolution, we account for transitions between coupled and decoupled states. For instance, strong updrafts can swiftly elevate convective clouds beyond the PBLH, creating a decoupled condition even when the cloud's properties still indicate a coupled situation. We have included an additional step to identify clouds that are adjunctly coupled to the surface using the CTH. If a cloud is found to be decoupled, we verify if it was in a coupled state in the previous time step (t–10 min). If so, we define it as a coupled case when the current CBH is below the previous CTH. This approach is based on the fact that, during rapidly growing convection, a cloud that was diagnosed as coupled at t–10 min can appear "decoupled" at time t under a snapshot CBH–PBLH criterion because the cloud (and/or the retrieved PBLH) can change quickly over 10 min. If the cloud was coupled one step earlier and its current base still lies below the altitude range occupied by the cloud in the previous step (as indicated by CBH(t) < CTH(t–10 min)) that suggests that the cloud has not fully detached into a new elevated layer; instead, it is more consistent with a transient growth/transition where the cloud deepens rapidly while remaining linked to the near-surface/PBL environment on that short timescale. This approach to identifying coupling considers the dynamic nature of cloud development and movement and acknowledges the transient nature of atmospheric processes.

2.3. Methodology for Assessing Aerosol-Deep Convective Cloud Interactions

Understanding ACI requires the observation of cloud lifetime and evolution. However, fixed ground-based observations can only capture screenshots of the cloud at the moment when clouds pass over the sensor. With such a limitation, observational studies based on ground-based data rely on statistical approaches that measure different stages of a cloud at different times. The ARM cloud type classification product divides clouds into seven categories, from which only three can potentially be coupled to the surface: low clouds, congestus, and deep convective. For doing such a classification, the cloud-type product depends exclusively on cloud boundaries (cloud base and height). Therefore, selecting only cases classified as DCCs would only provide a sample of well-mature clouds, hindering our understanding of the impact of aerosols on the life cycle of DCCs, at least from early to late stages of cloud development. Following this idea, we took all clouds classified as low clouds, congestus, and deep convection in the cloud type product instead of only those classified as DCCs. This approach, however, has its own limitations. For example, contamination from low clouds does not develop into convective systems. One way to mitigate this problem is by constraining meteorological conditions that facilitate convection. We also constrained our sample to only cases where the average daytime LNB < -4°C.

The PBLH retrievals were determined using the DTDS algorithm (Roldán-Henao et al., 2024; Su et al., 2020). These retrievals are available at a 10-min temporal resolution and are only accessible for daytime hours, since PBLH retrieved from Micropulse LiDAR (MPL) tends to be mis-identified due to the presence of residual layers, especially at night when PBL is generally low due to weak turbulence. As a result, all the variables we studied were resampled to a 10-min interval, and the analysis was limited to the period from 6:00 a.m. to 6:00 p.m. The CAPE was computed using the thermodynamic profiles of the mergesonde products. In our CAPE estimations, we observed that some retrievals were much higher than 5,000 J/kg, which, although possible, are rare and might be due to uncertainties in the mergesonde product. For our analysis, we considered CAPE values between 0 and 5,000 J/kg. Additionally, we noted that CAPE is mostly 0 J/kg during the cold months between November and February. This is a period when the atmosphere is typically stable, hindering local convection, which is not the main focus of the invigoration effect. Consequently, we decided to analyze only the months between March and October, during which local convection is more favorable. After completing the data preprocessing, we categorized our data set into coupled and decoupled clouds. Subsequently, we analyzed the impact of cloud-surface coupling and CAPE on aerosol-DCC interactions, following a methodology similar to Li et al. (2011) and Varble18. This involved categorizing the data into six CN categories ranging from 0 to 6,000 cm^{-3}. Finally, as Li et al. (2011) and Varble (18), we evaluate the uncertainty in our estimations using the standard error of the mean (SEM). The SEM indicates how much the mean of our sample may differ from the true population mean. It is calculated using the formula $SEM = \sigma/\sqrt{n}$, where σ is the standard deviation and n is the number of samples.

2.4. Assessment of Large-Scale Patterns and Different Air Mases Influence

To evaluate the correlation between CAPE and aerosols, we analyzed large-scale synoptic patterns using hourly ERA5 reanalysis data. For this analysis, we gathered 20 years of geopotential height and temperature records across the continental U.S. and calculated the anomalies using a Z-score technique. The anomalies for both coupled and decoupled cases were examined during clean conditions (CN ranging from 0 to 1,000 cm^{-3}) and polluted conditions (CN ranging from 5,000 to 6,000 cm^{-3}). The data of cloud-surface coupling classification are resampled to a one-hour resolution to align with the ERA5 reanalysis data. In the final analyses, our ACI analysis is repeated based on the origin of air masses. We differentiated between air coming from the south and air coming from the north according to 12-hr mean wind direction.

3. Results

According to Roldán-Henao et al. (2026), on average, around 66% of clouds at the SGP site are coupled with the PBLH, while the rest are decoupled. These fractions are not static but fluctuate throughout the day, with coupled clouds starting at less than 60% in the morning and peaking at around 80% in the afternoon (15 LST). This increase in coupled clouds is associated with the growth of the PBLH driven by variations in surface sensible heat fluxes (Zhang et al., 2024). As the PBLH deepens, more clouds become coupled to the surface or are formed aloft. Later in the day, as thermal activity subsides, lifted clouds may decouple from the PBLH, leading to a decrease in the percentage of coupled clouds.

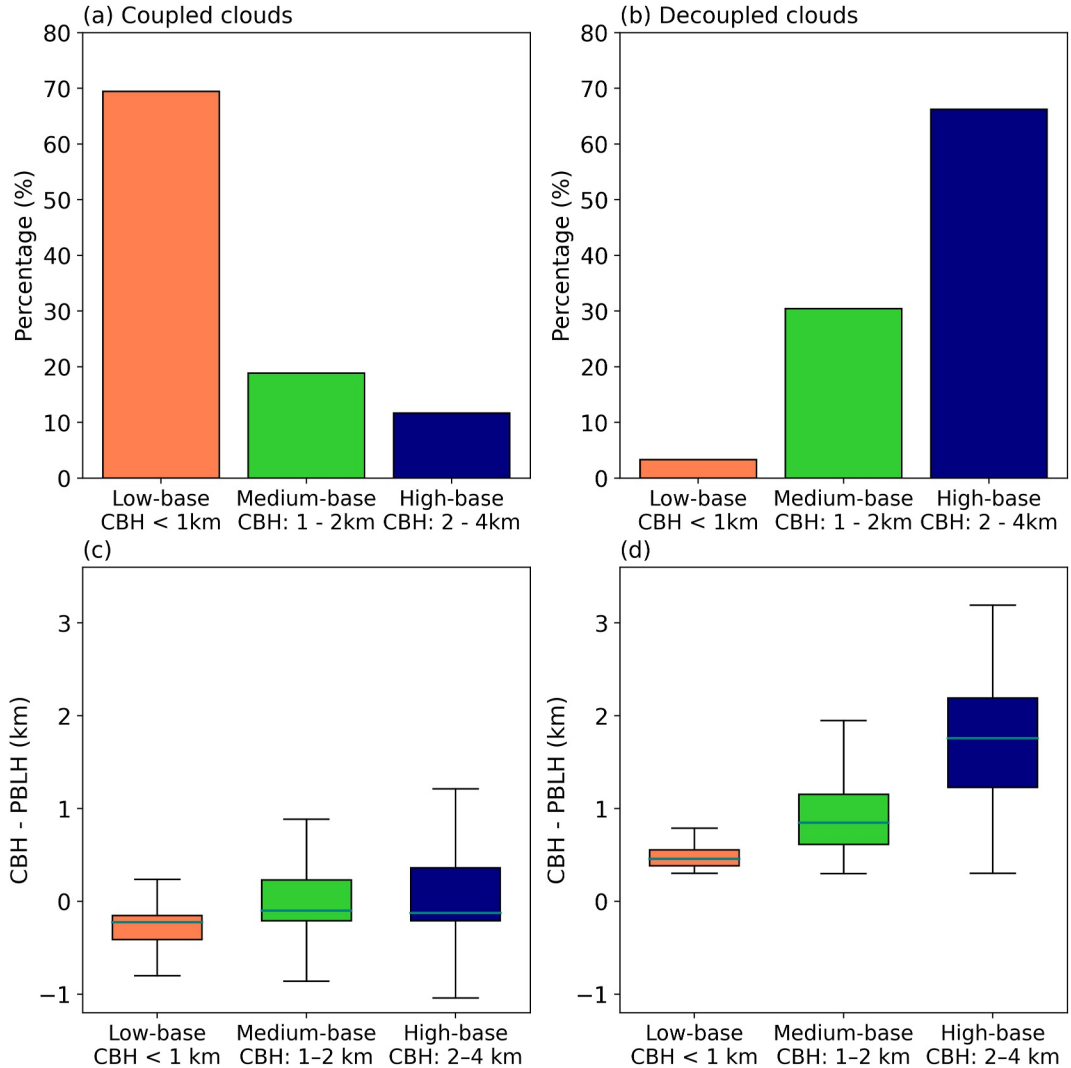

Figure 2. (a) Percentages of coupled clouds with bases below 1 km (orange bar), between 1 and 2 km (green bar), and between 2 and 4 km (blue bar). (b) Same as (a) but for decoupled clouds. (c) Boxplot for the difference between the cloud base height (CBH) and the planetary boundary layer height (PBLH) for coupled clouds with CBH below 1 km (orange bar), between 1 and 2 km (green bar), and between 2 and 4 km (blue bar). The teal horizontal lines correspond to the median values. (d) Same as (c) but for coupled clouds.

The coupling between clouds and the PBL is strongly influenced by the CBH. Figures 2a and 2b categorize clouds into three groups based on their base heights, as was done in Li et al. (2011), but for more data samples: low-base corresponding to clouds with CBH < 1 km, medium-base clouds as those with CBH between 1 and 2 km, and high-base clouds with CBH between 2 and 4 km, for both coupled and decoupled conditions that differ from Li et al. (2011). As seen in Figure 2a, clouds of lower bases are more likely coupled, with approximately 65% of coupled clouds located below 1 km. Figures 2c and 2d illustrate the difference between CBH and PBLH using a boxplot that represents the data distribution. Negative CBH–PBLH values imply that cloud bases reside within the PBL, allowing surface fluxes to influence cloud development. In contrast, positive differences indicate that clouds form above the PBL, suggesting reduced surface influence and a higher likelihood of decoupling. A clear height dependence emerges: as CBH increases, clouds are more frequently found above the PBL, especially under decoupled conditions, whereas in the coupled scenario, cloud bases consistently reside within or close to the PBL top, maintaining close linkage with the surface. Notably, about 60% of decoupled clouds are above 2 km. They tend to have a significant separation from the PBLH, with an average CBH-PBLH difference exceeding 1.5 km (Figure 2d). In the case of coupled clouds, nearly 70% have bases below 1 km, with the entire interquartile range of CBH-PBLH difference being negative.

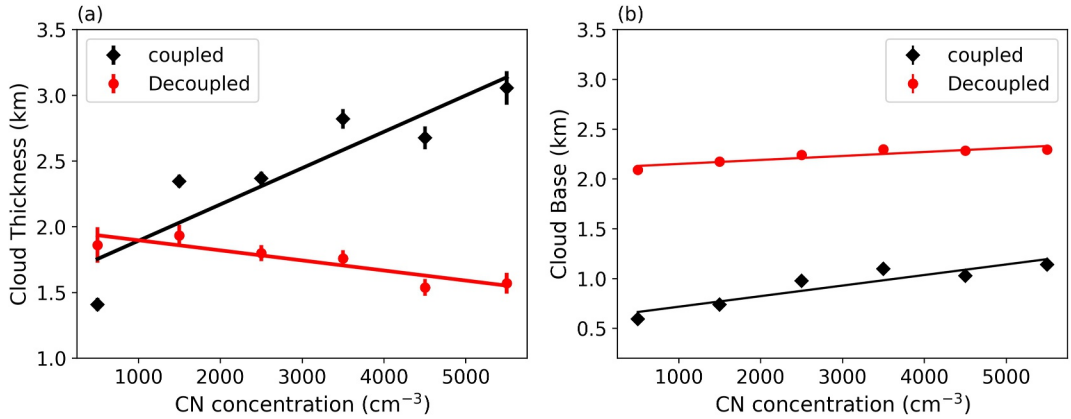

Figure 3. (a) Changes in the cloud geometrical thickness with the aerosol number concentration (CN) for coupled (black) and decoupled (red) conditions. (b) Changes in the cloud base height with the aerosol number concentration for coupled (black) and decoupled (red) conditions. Vertical lines correspond to the standard error of the mean.

Following Li et al. (2011), we aim to examine whether and how changes in aerosol number concentration affect the cloud geometrical thickness. However, unlike Li et al. (2011), we categorized our samples into coupled and decoupled conditions with 8 years more of data from 1998 to 2016 for all analyses, except for those analyses involving CAPE, which are limited to the period between 1999 and 2015 due to the availability of the mergesonde product. The results shown in Figure 3 are similar to the findings of Li et al. (2011), showing a positive correlation between aerosol number concentration and cloud thickness. As aerosol concentration increases from 500 to 6,500 cm^{-3}, cloud top increases about 1,300 m under coupled conditions and slightly decreases under decoupled conditions. There might be multiple reasons for this difference. One reason is that coupled clouds are inherently more influenced by surface heat, moisture, and aerosol loading due to their proximity to the boundary layer. These factors are crucial for cloud development and evolution, making coupled clouds more susceptible to aerosols. Another reason is that, as explained by Su et al. (2024), the vertical aerosol structure differs between coupled and decoupled regimes, with coupled conditions exhibiting a more uniform distribution in the vertical profile of aerosol concentration between the surface and cloud base. In contrast, decoupled clouds have a more stratified structure between the surface and the cloud base. This difference in aerosol vertical distribution allows surface aerosol measurements to serve as a more reliable proxy of CCN, the root of the ACI under coupled conditions but not under decoupled conditions.

For the same range of change in CN concentration, the cloud base rises slightly, about 500 and 300 m for both coupled and decoupled clouds. Based on the invigoration effect, aerosols enhance convective updrafts, resulting in increases in cloud top heights and, consequently, greater cloud thickness. The slight increase could be attributed to the influence of varying air masses. Specifically, higher aerosol loadings are associated with advection from the south, bringing warmer, moister, and more polluted air, which favors elevated cloud bases, while clean, colder air masses from the north lead to lower cloud bases. Such influence of varying air masses is also the reason for the CAPE-aerosol correlation. We will discuss this point later.

Figure 4a shows the changes in cloud thickness of coupled clouds with CN concentration for various cloud base categories. The most notable increase is seen for coupled clouds with bases below 1 km, where cloud thickness increases approximately 3 km when aerosol concentration rises from 500 to 5,500 cm^{-3}. For medium-base coupled clouds, the increase in thickness is more modest, with an increment of roughly 700 m within the same range of aerosol concentration. Conversely, high-base coupled clouds virtually show no change in thickness with varying aerosol concentration. The positive linear trends observed for both low-base and medium-base coupled clouds are statistically significant at the 0.05 level, according to the Wald Test and the *F*-test. Based on the theoretical basis, two plausible reasons explain the larger ACI effect observed for lower-base clouds. First, the distance between the cloud base and the melting level would be larger, allowing much more warm rain to form through enhanced collision processes compared to high cloud base clouds. This effect will strongly mediate the freezing-induced invigoration. Second, condensation is much greater at lower altitudes due to higher specific

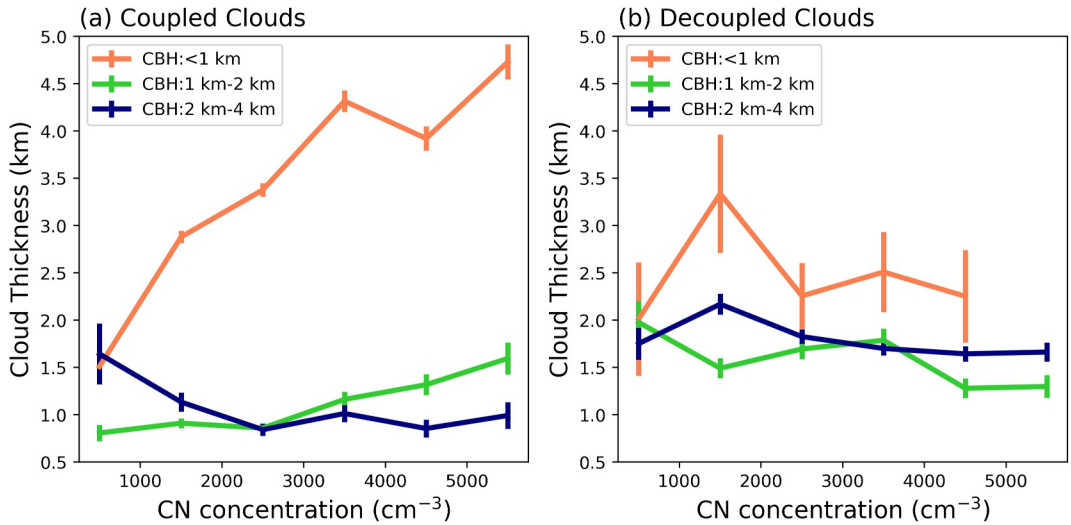

Figure 4. (a) Changes in the cloud geometrical thickness with the aerosol number concentration (CN) for coupled clouds with bases below 1 km (orange line), between 1 and 2 km (green line), and between 2 and 4 km (blue line). (b) Same as (a) but for decoupled clouds. Vertical lines correspond to the standard error of the mean.

humidity. As a result, the heating from condensation can be significantly greater when compared to clouds with higher bases, leading to a larger degree of condensational invigoration.

In contrast to coupled clouds, decoupled clouds show no visible relationship between cloud thickness and aerosol concentration regardless of CBH (Figure 4b). The features as shown in Figure 4a are principally the same as Li et al. (2011), but no differentiation was made with regard to the state of cloud-surface coupling, which turns out to be a key influential factor. This similarity bears out the fact that coupled clouds account for about two-thirds of warm clouds. However, its proportion increases with decreasing CBH (Roldán-Henao et al., 2026).

Following Varble18's findings on the correlations between CAPE and CN concentration, we conducted a sensitivity analysis by studying the relationship between the cloud thickness and the CN concentration under the constraint of CAPE, LNB, and LFC values. This approach provides a better understanding of how changes in meteorology influence the relationship between aerosol loading and cloud thickness. Figures 5a and 5b show the relationship between the cloud thickness and the CN concentration for (a) low-base coupled clouds and (b) medium-base coupled clouds for different CAPE percentiles. Coupled clouds of high-base were excluded due to too few samples in this category. Figures 5c and 5d depict the changes in CBH with CN concentration, suggesting that changes in cloud thickness are primarily driven by changes in the cloud top. Figure 5a shows consistent increases in cloud thickness with CN concentration for all clusters of CAPE's percentiles. In particular, low-level coupled clouds thicken between 1 and 4 km, depending on the CAPE percentile. The positive correlations between cloud thickness and CN concentration are statistically significant based on the Wald-test and the *F*-test at the 0.05 level for nearly all CAPE percentiles, except for the first percentile (represented by the blue line), which has a p-value of 0.13. It is important to note that both CAPE and aerosols affect cloud development. Not surprisingly, the slope of the increase correlates with CAPE: steeper for higher CAPE than for lower CAPE. One may thus conclude that the substantial increase in cloud thickness observed in low-base coupled clouds is not solely attributed to variations in CAPE, but to both the impacts of CAPE and the aerosol invigoration effect. Finally, Figures 5e and 5f illustrate how CAPE varies with aerosol concentration for each percentile for low and medium cloud bases respectively, under coupled conditions. Contrary to cloud thickness, CAPE remains relatively constant, further suggesting that aerosols might play a role in invigorating clouds under coupled conditions. Figures S1 and S2 in Supporting Information S1 show the same analysis but for LNB and LFC, respectively. Similar conclusions are observed, with cloud thickness increasing with aerosol loading for different percentiles of the meteorological variables.

In the case of medium-base coupled clouds, our sample size is limited to about 25% (Figure 1a) of the total number of coupled clouds. Given the fewer samples, we segmented the analysis into only 3 CAPE percentiles. As mentioned earlier, the strength of coupling is less significant for medium-base clouds compared to low-base

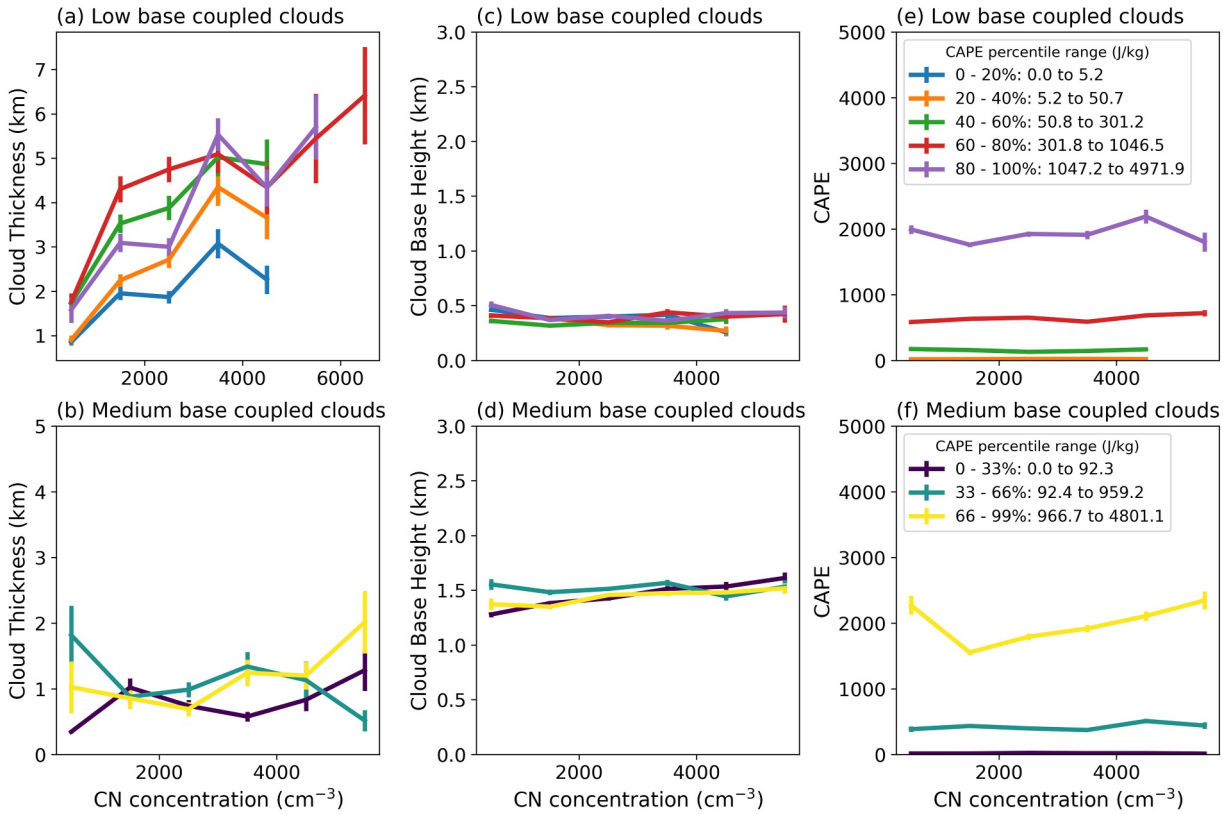

Figure 5. Cloud thickness variations with aerosol number (CN) concentration for different convective available potential energy (CAPE) percentiles for (a) low-base coupled clouds and (b) medium-base coupled clouds. Cloud base height variations with CN concentration for different CAPE percentiles for (c) low-base coupled clouds and (d) medium-base coupled clouds. CAPE variations with aerosol concentration for the different CAPE percentiles for (e) low-base coupled clouds and (f) medium-base coupled clouds. For each aerosol and CAPE interval, mean values are shown only when the sample size exceeds 20. Vertical lines correspond to the standard error of the mean.

clouds, making the aerosol-clouds interaction estimate less significant. Moreover, due to the fewer samples, the analysis for this cloud type is less robust compared to that for low-base clouds. Figure 5d shows an increasing trend in cloud thickness only for the last CAPE percentile (yellow line), which is statistically significant. However, we can also observe an increasing trend in CAPE when the aerosol loading increases from 1,500 to 5,500 cm^{-3}, which complicates the separation between meteorology and aerosols in this case.

Similar to Figures 5 and 6 shows the sensitivity analysis of CAPE for the relationship between cloud thickness and CN concentration under decoupled conditions for (a) medium-medium- and (b) high-base clouds. The analysis on Low-base clouds is omitted, given the limited sample size for this category (Figure 2b). Overall, no distinct trend emerges between cloud thickness and CN concentration across any CAPE percentile or CBH, and none of the observed relationships is statistically significant. However, this doesn't mean that decoupled clouds are insensitive to aerosol concentration. This is just the reflection of using surface-based aerosol measurements that don't represent cloud base concentrations. The only consistent pattern is the expected relationship between cloud thickness and CAPE; the higher the thickness, in accordance with the fundamentals of cloud physics.

The strong dependence on aerosol loading for coupled clouds and little dependence for decoupled clouds imply that the state of coupling is another key variable when studying the aerosol invigoration effect based on ground-based measurements, which is something has not been noted before. Figures S3 and S4 in Supporting Information S1 show the same analysis as Figure 5 but for the LNB and LFC, respectively.

As mentioned in the introduction, Varble18 found a positive relationship between CAPE and aerosol loading and thus argued that it is CAPE that ultimately drives the cloud development. An attempt was made to find the cause of such a positive relationship by analyzing the mean synoptic conditions in terms of geopotential height and temperature. It was found that dirty conditions are associated with higher surface temperatures and a stronger

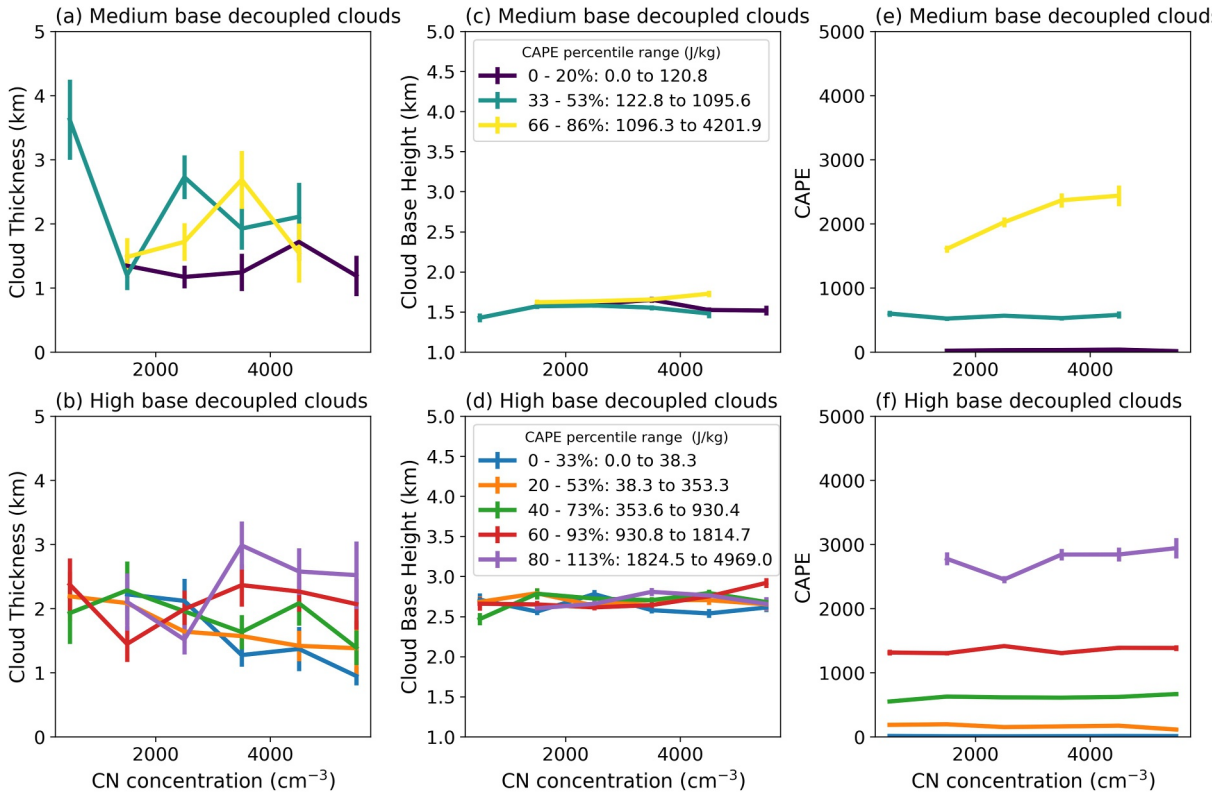

Figure 6. Cloud thickness variations with aerosol number (CN) concentration for different convective available potential energy (CAPE) percentiles for (a) medium-base decoupled clouds and (b) high-base decoupled clouds. Cloud base height variations with CN concentration for different CAPE percentiles for (c) medium-base decoupled clouds and (d) high-base decoupled clouds. CAPE variations with aerosol concentration for the different CAPE percentiles for (c) medium-base decoupled clouds and (f) high-base decoupled clouds. For each aerosol and CAPE interval, mean values are shown only when the sample size exceeds 20. Vertical lines correspond to the standard error of the mean.

south-southwesterly flow compared with clean conditions, which exhibit colder temperatures and an anomalous upper-level northerly flow. However, Varble18 concluded that the magnitude of these differences may be small enough to be comparable to measurement errors. Following the Varble18 attempt, we analyzed the synoptic-scale patterns at 850 hPa for clean conditions ($0 < CN < 1{,}000$ cm^{-3}) and dirty conditions ($4{,}000 < CN < 5{,}000$ cm^{-3}), but we further divided our analyses for coupled and decoupled clouds and instead of using mean values, we analyzed the climatological anomalies.

Figure 7 presents the results of the synoptic-scale analysis. Under coupled clean conditions (Figure 7a), surface temperatures around the SGP site (yellow star) are lower, as indicated by the blue shading. We also observed anomalous northerly winds, associated with lower geopotential heights to the east of Oklahoma and higher geopotential heights to the northwest. In coupled dirty conditions (Figure 7c), the anomalies are generally weaker than in clean conditions. Under dirty coupled conditions, winds originate from the south, transporting warmer, more humid air masses that may carry both marine aerosols and aerosols from Texas. Not surprisingly, these findings for coupled conditions align with those reported by Varble18, as coupled cases account for 70% of the sample, thereby dominating the mean state.

In decoupled scenarios, the findings do not completely align with those of Varble18. While surface temperatures around the SGP site remain lower under clean conditions, the anomalies are somewhat less pronounced. The most notable differences between coupled and decoupled conditions manifest in the geopotential height field. In clean decoupled conditions (Figure 7b), the geopotential height contour lines are more spread-out, indicating weaker wind patterns. Furthermore, the signal of anomalous lower geopotential height observed in Figure 7a seems to have shifted westward, now centering near the SGP site. Consequently, the winds should exhibit a stronger easterly component compared to clean coupled scenarios. In decoupled dirty conditions, the anomalies are weakest, approaching zero, with no significant patterns.

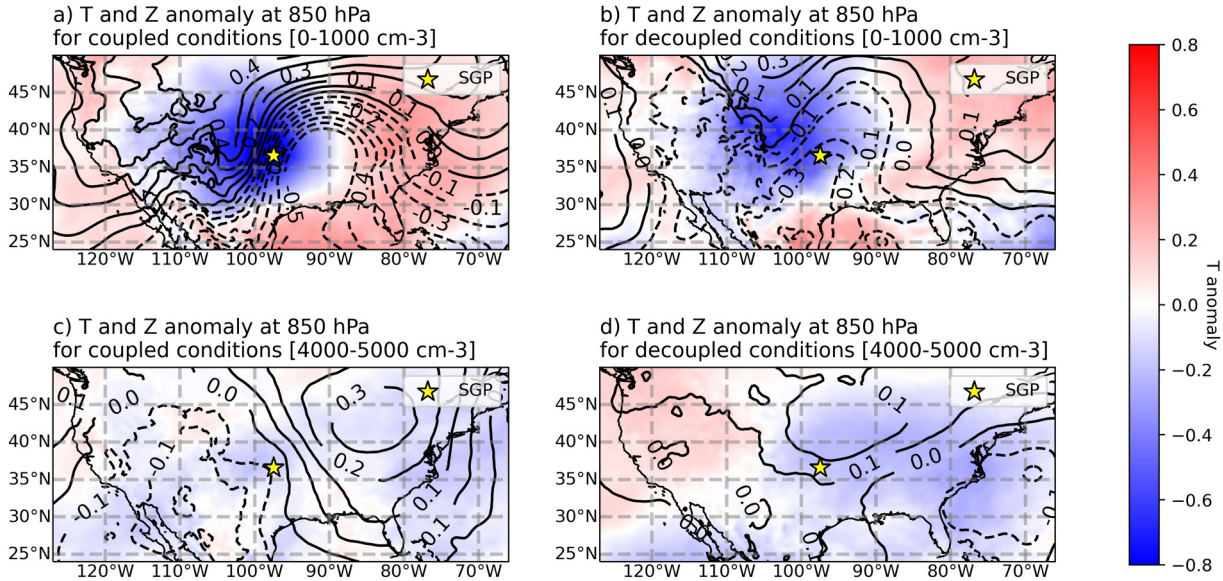

Figure 7. ERA5 climatological anomalies at 850 hPa for temperature (T) (shaded) and geopotential height (Z) (black contour lines). Positive Z anomalies are shown with solid black lines, while negative Z anomalies are represented with dashed lines. The yellow star marks the Southern Great Plains site location. (a) Anomalies for coupled clean conditions, (b) anomalies for decoupled clean conditions, (c) anomalies for coupled dirty conditions, and (d) anomalies for decoupled dirty conditions.

Since the positive relationship between CAPE and aerosol is likely explained by the origin of air masses, we further constrain the influence of meteorology by categorizing air masses based on their origin—either from the south or the north. This separation allows us to minimize the confounding effects of CAPE–aerosol co-variability. We separated the air masses by computing the mean wind direction over the 12 hr preceding each cloud measurement and classifying winds as either northerly or southerly. Figure 8 presents an analysis similar to Figure 3 but differentiates between these two wind regimes. The same trend is seen: an increase in cloud thickness with aerosol concentration is observed only under coupled conditions. Interestingly, the rate of this increase is steeper for northerly winds than for southerly winds. Overall, northerly winds show an increase of approximately 2 km when CN increases from 500 cm to 3 to 5,500 cm^{-3}, whereas southerly winds only increase approximately 500 m for the same aerosol range. One possible explanation for the difference is that northern air masses tend to be cleaner than southern ones, as shown in Figure 7. This suggests that northern air masses represent an aerosol-limited environment, where variations in aerosol loading strongly influence cloud properties. In contrast, southern air masses likely contain higher baseline aerosol concentrations, meaning that additional aerosol loading has a more muted impact on cloud development.

Finally, a similar analysis as Figure 5 was conducted to investigate the ACI by segregating the effects of air mass separated by northly and southerly winds, atmospheric stability denoted by CAPE, and the state of cloud-PBL coupling. Given the limited sample size, the analysis is constrained to three CAPE percentiles instead of five. The results are illustrated in Figure 9. Panel (a) shows a general increase in cloud thickness across different CAPE percentiles for coupled clouds with air masses from the south. However, this trend is statistically significant only for the last CAPE percentile of 66%–99%, where the increase is more pronounced. For coupled clouds with air masses from the north (panel d), cloud thickness also increases across different CAPE percentiles, with a steeper slope between 0 and 2,500 cm^{-3}. Our analysis shows statistical significance for the second CAPE percentile (33%–66%). It is important to mention that, given the numerous constraints applied to the data in Figure 9, statistical significance in these analyses is relatively low. Figures S5 and S6 in Supporting Information S1 display the same analysis for the LNB and LFC; similar trends are observed with increases in cloud thickness with the aerosol concentration for different percentiles of these two meteorological variables.

4. Summary and Discussion

This investigation revisits the previous findings of Li et al. (2011) on the aerosol invigoration effect and addresses a concern raised by Varble (2018). Li et al. (2011) found a positive correlation between aerosol concentration and

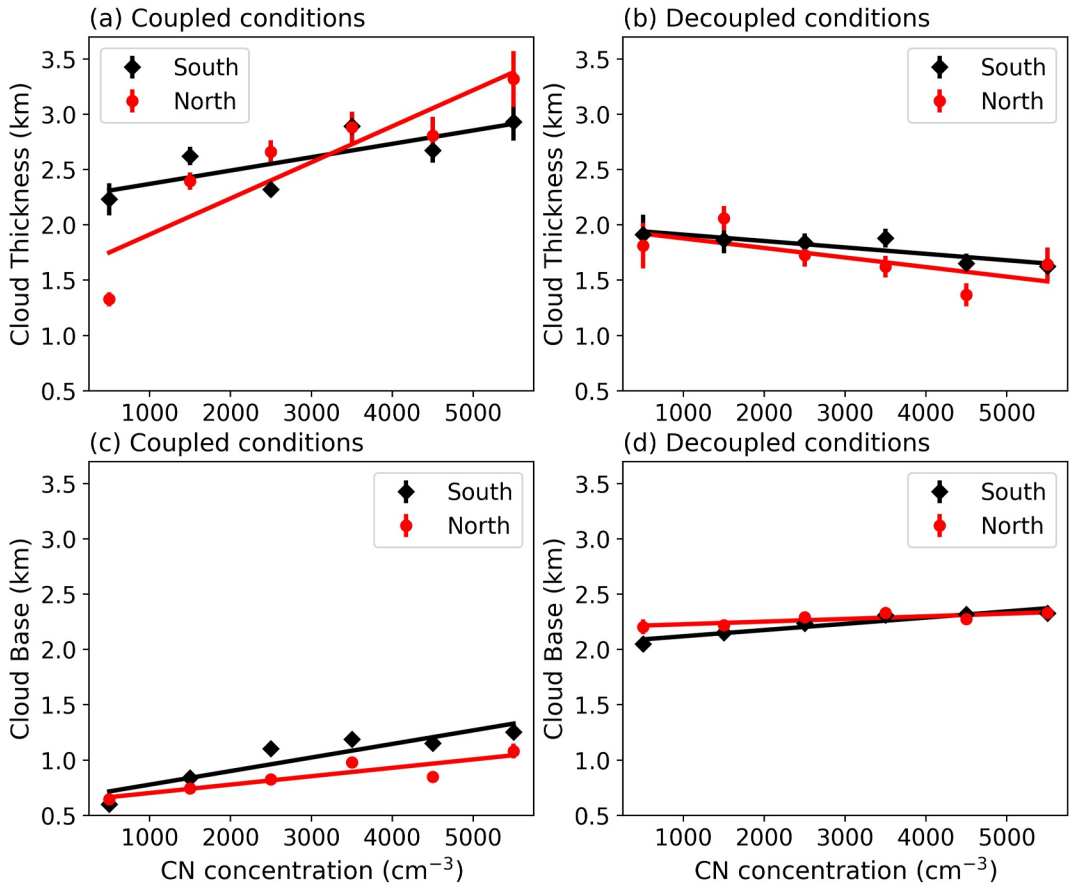

Figure 8. Variations in cloud geometrical thickness (a)–(b) and cloud base height (c)–(d) as a function of aerosol number concentration (CN) under coupled and decoupled conditions. Red lines represent air masses originating from the north, while black lines correspond to air masses from the south. Panels (a) and (c) show results for coupled conditions, whereas panels (b) and (d) correspond to decoupled conditions. Vertical lines correspond to the standard error of the mean.

cloud thickness and suggested that increased aerosols can enhance cloud development. Finding a positive correlation between aerosols and CAPE, Varble (2018) argued that the enhanced cloud development could be caused by the co-variability between CN concentration and CAPE. A more rigorous evaluation is made here of the underlying mechanisms behind the findings of Li et al. (2011), which is becoming feasible as the needed observation samples have expanded considerably, together with new capability enabled by the availability of cloud-PBL coupling (Roldán-Henao et al., 2026), which has been demonstrated to play a key role in studying the ACI using ground-based measurements (Su et al., 2024).

We have thus expanded the analysis to cover at least 16 years (November 1998–June 2015) of ARM data, with some analyses extending to 17 years. The expanded data volume helps lower sampling errors and allows for more in-depth analyses and disentangling the roles of aerosols from meteorology. First, to examine whether aerosol measurements made on the ground are a valid proxy for aerosol near the cloud base, we resort to the concept of cloud-surface coupling. Coupling allows for a more accurate assessment of ACI, as it ensures that ground-based aerosol measurements reliably represent the aerosols involved in cloud formation and development—a challenge that has long complicated ACI studies (Quaas et al., 2020). We found the same positive relationship between aerosol concentration and cloud thickness only for coupled clouds, with an overall increase in cloud thickness that varies between 1 and 4 km depending on the CAPE percentile. Under coupled situations, ground-based measurements are a valid proxy of aerosols participating in the ACI processes. By contrast, little dependence is found for decoupled clouds.

Secondly, to isolate the aerosol effect from the CAPE effect, we conducted a sensitivity analysis to understand how the correlation found by Varble (2018) between CN and CAPE affects the relationship between aerosols and

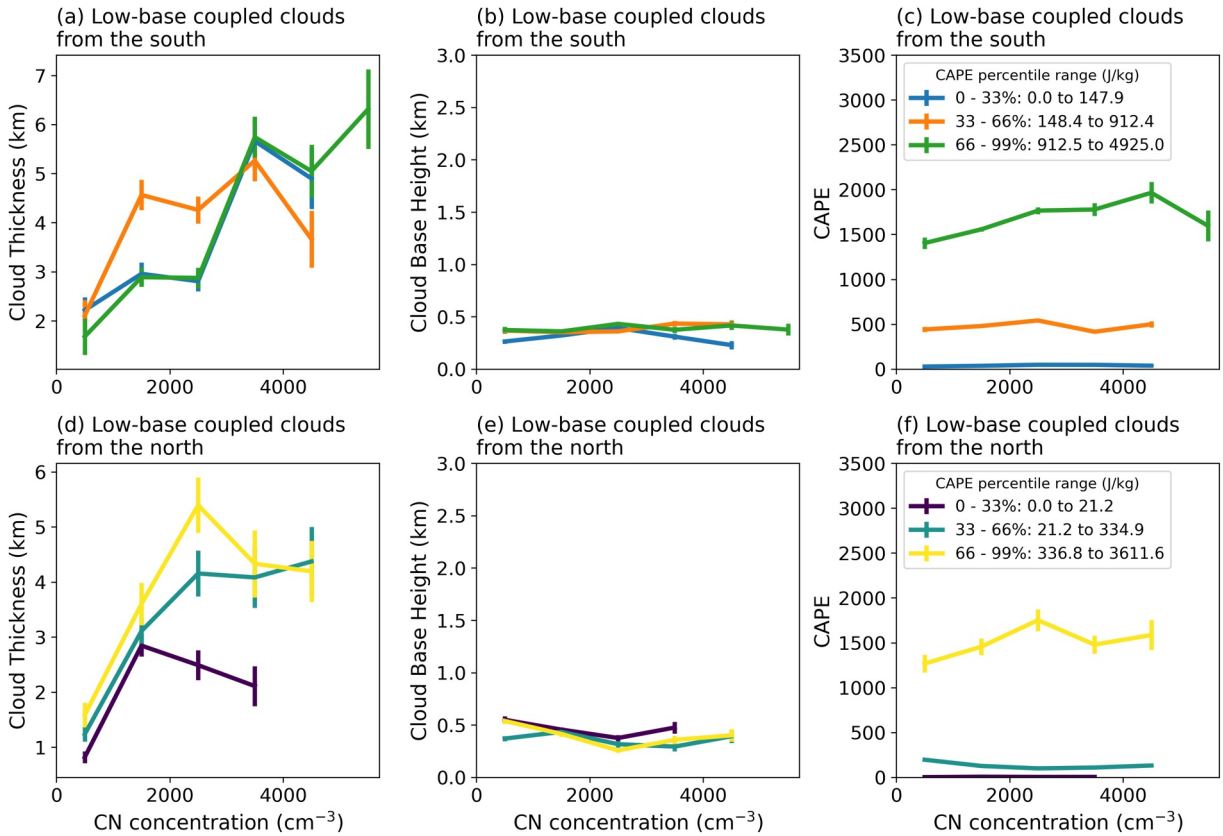

Figure 9. Cloud thickness variations with aerosol number (CN) concentration for different convective available potential energy (CAPE) percentiles for (a) low-base coupled clouds from the south and (d) low-base coupled clouds from the north. Cloud base height variations with CN concentration for different CAPE percentiles for (b) low-base coupled clouds from the south and (e) low-base coupled clouds from the north. CAPE variations with aerosol concentration for the different Level of Neutral Buoyancy (LNB) percentiles for (c) low-base coupled clouds from the south and (f) low-base coupled clouds from the north. For each aerosol and LNB interval, mean values are shown only when the sample size exceeds 20. Vertical lines correspond to the standard error of the mean.

cloud thickness. To this end, we binned the data samples into percentile ranges of CAPE and analyzed the relationship within each range. Positive correlations between CN and cloud thickness persist across all percentiles only for coupled low base clouds. Moreover, the slope of the relationship is steeper for higher CAPE, attesting to its role in strengthening convective clouds. Similar relationships were found when this analysis was repeated for the LNB and LFC.

Thirdly, we investigate the co-variability between aerosol loading and CAPE. Consistent with Varble (2018), our analysis indicates that clean cases are predominantly associated with northerly air masses, while dirty conditions are linked to southerly air masses. However, this pattern was only evident in coupled conditions. This finding, derived from almost two decades of data, indicates that the observed positive correlation between CAPE and aerosols is largely explained by the distinct characteristics of these air masses: cold and clean from the north versus warm and polluted from the south. Notably, changes in cloud thickness in response to aerosol concentration were more pronounced under northerly (cleaner) wind regimes, suggesting a potentially aerosol-limited environment that could amplify the invigoration effect within cleaner background air.

The aforementioned findings suggest that the positive relationship reported by Li et al. (2011) is unlikely to be solely caused by co-variability between CAPE and CN. More likely, both CAPE and aerosols contribute to the development of convective clouds, together with other factors such as weather regime, surface forcing, and wind shear.

However, caution should be exercised in interpreting the findings, as they are based on a single-site measurements and may not generalize across different climate regimes. Additionally, some uncertainties in this observational study could influence the results. For instance, the use of surface aerosol data (although partially mitigated by

including cloud-surface coupling) might be problematic. Furthermore, the study does not account for aerosol size and composition, despite other research suggesting that fine or ultrafine aerosols have different effects compared to coarse aerosols. The observations of cloud development also come with significant uncertainties due to the limitations of LiDAR and radar instruments. Moreover, the methodology and data used in this investigation do not clarify whether the invigoration signal observed is due to freezing or condensational invigoration, or a combination of both. However, based on our findings, we conclude that the invigoration effect is plausible, particularly under the conditions of high CAPE and clean background.

Conflict of Interest

The authors declare no conflicts of interest relevant to this study.

Availability Statement

All ARM data at five sites are publicly available at the USA DOE ARM Data Center: CLDTYPE: https://www.arm.gov/data/science-data-products/vaps/cldtype (Zhang et al., n.d.), AOS: https://www.arm.gov/capabilities/instruments/aos (Mayol Bracero et al., n.d.), and MERGESONDE: https://www.arm.gov/data/science-data-products/vaps/mergesonde (Wang et al., n.d.-a; n.d.-b). The PBL height derived from DTDS over the SGP can be downloaded from https://doi.org/10.5281/zenodo.7374849 (Su, 2022). ERA5 temperature and geopotential height data are publicly available at the Copernicus Climate Change Service: https://cds.climate.copernicus.eu/datasets/reanalysis-era5-single-levels?tab=overview (Hersbach et al., 2023).

Acknowledgments

NRH and ZL were supported by the U.S. Department of Energy Office of Science's Biological and Environmental Research Atmospheric System Research under Award Number DE-SC0022919 and the National Science Foundation (AGS2126098 and AGS2534194). NRH was in part funded by NASA (80NSSC21K1980). JEY was funded by the NASA Earth Science Division Radiation Sciences program. TS work at LLNL is performed under the auspices of the U.S. Department of Energy by LLNL under Contract DE-AC52-07NA27344. JF was supported by the U.S. Department of Energy's Atmospheric System Research, an Office of Science Biological and Environmental Research program; Argonne National Laboratory is operated for the DOE UChicago Argonne, LLC, under contract DE-AC02-06CH11357.

References

Abbott, T. H., & Cronin, T. W. (2021). Aerosol invigoration of atmospheric convection through increases in humidity. *Science*, *371*(6524), 83–85. https://doi.org/10.1126/science.abc5181

Andreae, M. O., Rosenfeld, D., Artaxo, P., Costa, A. A., Frank, G. P., Longo, K. M., & Silva-Dias, M. A. F. (2004). Smoking rain clouds over the Amazon. *Science*, *303*(5662), 1337–1342. https://doi.org/10.1126/science.1092779

Berg, L. K., & Stull, R. B. (2005). A simple parameterization coupling the convective daytime boundary layer and fair-weather cumuli. *Journal of the Atmospheric Sciences*, *62*(6), 1976–1988. https://doi.org/10.1175/JAS3437.1

Betts, A. K. (2009). Land-surface-Atmosphere coupling in observations and models. *Journal of Advances in Modeling Earth Systems*, *1*(3), 4. https://doi.org/10.3894/james.2009.1.4

Bretherton, C. S., & Wyant, M. C. (1997). Moisture transport, lower-tropospheric stability, and decoupling of cloud-topped boundary layers. *Journal of the Atmospheric Sciences*, *54*(1), 148–167. https://doi.org/10.1175/1520-0469(1997)054<0148:MTLTSA>2.0.CO;2

Brotzge, J. A., & Richardson, S. J. (2003). Spatial and temporal correlation among Oklahoma mesonet and OASIS surface-layer measurements. *Journal of Applied Meteorology*, *42*(1), 5–19. https://doi.org/10.1175/1520-0450(2003)042<0005:satcao>2.0.co;2

Clothiaux, E. E., Ackerman, T. P., Mace, G. G., Moran, K. P., Marchand, R. T., Miller, M. A., & Martner, B. E. (2000). Objective determination of cloud heights and radar reflectivities using a combination of active remote sensors at the ARM CART sites. *Journal of Applied Meteorology*, *39*(5), 645–665. https://doi.org/10.1175/1520-0450(2000)039<0645:odocha>2.0.co;2

Cotton, W. R., & Walko, R. (2021). Examination of aerosol-induced convective invigoration using idealized simulations. *Journal of the Atmospheric Sciences*, *78*(1), 287–298. https://doi.org/10.1175/JAS-D-20-0023.1

Dong, X., Schwantes, A. C., Xi, B., & Wu, P. (2015). Investigation of the marine boundary layer cloud and CCN properties under coupled and decoupled conditions over the azores. *Journal of Geophysical Research*, *120*(12), 6179–6191. https://doi.org/10.1002/2014JD022939

Ek, M. B., & Holtslag, A. A. M. (2004). Influence of soil moisture on boundary layer cloud development. *Journal of Hydrometeorology*, *5*(1), 86–99. https://doi.org/10.1175/1525-7541(2004)005<0086:IOSMOB>2.0.CO;2

Fan, J., & Li, Z. (2022). Aerosol interactions with deep convection. In K. Carslaw (Ed.), *Aerosols and climate*. Elsevier. Retrieved from https://www.sciencedirect.com/book/9780128197660/aerosols-and-climate

Fan, J., Rosenfeld, D., Ding, Y., Leung, L. R., & Li, Z. (2012). Potential aerosol indirect effects on atmospheric circulation and radiative forcing through deep convection. *Geophysical Research Letters*, *39*(9), L09806. https://doi.org/10.1029/2012GL051851

Fan, J., Rosenfeld, D., Zhang, Y., Giangrande, S. E., Li, Z., Machado, L. A. T., et al. (2018). Substantial convection and precipitation enhancements by ultrafine aerosol particles. *Science*, *359*(6374), 411–418. https://doi.org/10.1126/science.aan8461

Fan, J., Wang, Y., Rosenfeld, D., & Liu, X. (2016). Review of aerosol-cloud interactions: Mechanisms, significance, and challenges. *Journal of the Atmospheric Sciences*, *73*(11), 4221–4252. https://doi.org/10.1175/JAS-D-16-0037.1

Fan, J., Zhang, Y., Li, Z., Yan, H., Prabhakaran, T., Rosenfeld, D., & Khain, A. (2025). Unveiling aerosol impacts on deep convective clouds: Scientific concept, modeling, 2 observational analysis, and future direction. *Journal of Geophysical Research*, *130*, e2024JD041931. https://doi.org/10.1029/2024JD041931

Golaz, J. C., Larson, V. E., & Cotton, W. R. (2002). A PDF-based model for boundary layer clouds. Part I: Method and model description. *Journal of the Atmospheric Sciences*, *59*(24), 3540–3551. https://doi.org/10.1175/1520-0469(2002)059<3540:APBMFB>2.0.CO;2

Grabowski, W. W., & Morrison, H. (2021). Supersaturation, buoyancy, and deep convection dynamics. *Atmospheric Chemistry and Physics*, *21*(18), 13997–14018. https://doi.org/10.5194/acp-21-13997-2021

Hersbach, H., Bell, B., Berrisford, P., Biavati, G., Horányi, A., Muñoz Sabater, J., et al. (2023). ERA5 hourly data on single levels from 1940 to present [Dataset]. *Copernicus Climate Change Service (C3S) Climate Data Store (CDS)*. https://doi.org/10.24381/cds.adbb2d47

Hogan, R. J., Grant, A. L. M., Illingworth, A. J., Pearson, G. N., & O'Connor, E. J. (2009). Vertical velocity variance and skewness in clear and cloud-topped boundary layers as revealed by Doppler LiDAR. *Quarterly Journal of the Royal Meteorological Society*, *135*(640), 635–643. https://doi.org/10.1002/qj.413

Igel, A. L., & van den Heever, S. C. (2021). Invigoration or enervation of convective clouds by aerosols? *Geophysical Research Letters*, *48*(16), e2021GL093804. https://doi.org/10.1029/2021GL093804

Khain, A. P. (2009). Notes on state-of-the-art investigations of aerosol effects on precipitation: A critical review. *Environmental Research Letters*, *4*(1), 015004. https://doi.org/10.1088/1748-9326/4/1/015004

Khain, A. P., BenMoshe, N., & Pokrovsky, A. (2008). Factors determining the impact of aerosols on surface precipitation from clouds: An attempt at classification. *Journal of the Atmospheric Sciences*, *65*(6), 1721–1748. https://doi.org/10.1175/2007JAS2515.1

Koren, I., Dagan, G., & Altaratz, O. (2014). From aerosol-limited to invigoration of warm convective clouds. *Science*, *344*(6188), 1143–1146. https://doi.org/10.1126/science.1252595

Krishnamurthy, R., Newsom, R. K., Chand, D., & Shaw, W. J. (2021). *Boundary layer climatology at ARM Southern Great Plains (No. PNNL--30832)*. Pacific Northwest National Laboratory (PNNL).

Lebo, Z. J., & Morrison, H. (2014). Dynamical effects of aerosol perturbations on simulated idealized squall lines. *Monthly Weather Review*, *142*(3), 991–1009. https://doi.org/10.1175/MWR-D-13-00156.1

Li, Z., Lau, W. M., Ramanathan, V., Wu, G., Ding, Y., Manoj, M. G., et al. (2016). Aerosol and monsoon climate interactions over Asia. *Reviews of Geophysics*, *54*(4), 866–929. https://doi.org/10.1002/2015rg000500

Li, Z., Niu, F., Fan, J., Liu, Y., Rosenfeld, D., & Ding, Y. (2011). Long-term impacts of aerosols on the vertical development of clouds and precipitation. *Nature Geoscience*, *4*(12), 888–894. https://doi.org/10.1038/ngeo1313

Li, Z., Wang, Y., Guo, J., Zhao, C., Cribb, M. C., Dong, X., et al. (2019). East Asian study of tropospheric aerosols and their impact on regional clouds, precipitation, and climate (EAST-AIRCPC). *Journal of Geophysical Research: Atmospheres*, *124*(23), 13026–13054. https://doi.org/10.1029/2019jd030758

Liu, F., Mao, F., Rosenfeld, D., Pan, Z., Zang, L., Zhu, Y., et al. (2022). Opposing comparable large effects of fine aerosols and coarse sea spray on marine warm clouds. *Communications Earth & Environment*, *3*(1), 232. https://doi.org/10.1038/s43247-022-00562-y

Mayol Bracero, O., Springston, S., Andrews, E., Smith, S., & Campos de Oliveira, D. (n.d.). Aerosol observing system (NOAAAOS), 2007-05-19 to 2017-03-31, Southern Great Plains (SGP), central facility, Lamont, OK (C1) [Dataset]. *Atmospheric Radiation Measurement (ARM) User Facility*. https://doi.org/10.5439/1988399

Morrison, H., & Grabowski, W. W. (2013). Response of tropical deep convection to localized heating perturbations: Implications for aerosol-induced convective invigoration. *Journal of the Atmospheric Sciences*, *70*(11), 3533–3555. https://doi.org/10.1175/JAS-D-13-027.1

Münkel, C., Eresmaa, N., Räsänen, J., & Karppinen, A. (2007). Retrieval of mixing height and dust concentration with LiDAR ceilometer. *Boundary-Layer Meteorology*, *124*(1), 117–128. https://doi.org/10.1007/s10546-006-9103-3

Öktem, R., Romps, D. M., & Varble, A. C. (2023). No warm-phase invigoration of convection detected during GoAmazon. *Journal of the Atmospheric Sciences*, *80*(10), 2345–2364. https://doi.org/10.1175/JAS-D-22-0241.1

Quaas, J., Arola, A., Cairns, B., Christensen, M., Deneke, H., Ekman, A. M. L., et al. (2020). Constraining the Twomey effect from satellite observations: Issues and perspectives. *Atmospheric Chemistry and Physics*, *20*(23), 15079–15099. https://doi.org/10.5194/acp-20-15079-2020

Roldán-Henao, N., Su, T., & Li, Z. (2024). Refining planetary boundary layer height retrievals from micropulse-LiDAR at multiple ARM sites around the world. *Journal of Geophysical Research: Atmospheres*, *129*(13), e2023JD040207. https://doi.org/10.1029/2023JD040207

Roldán-Henao, N., Su, T., Li, Z., Zheng, Y., & Yorks, J. (2026). Climatology of cloud-land-surface coupling across different ARM sites. *Journal of Geophysical Research: Atmospheres*, *131*(1), e2025JD044010. https://doi.org/10.1029/2025jd044010

Rosenfeld, D., Lohmann, U., Raga, G. B., O'Dowd, C. D., Kulmala, M., Fuzzi, S., et al. (2008). Flood or drought: How do aerosols affect precipitation? *Science*, *321*(5894), 1309–1313. https://doi.org/10.1126/science.1160606

Stevens, B., & Feingold, G. (2009). Untangling aerosol effects on clouds and precipitation in a buffered system. *Nature*, *461*(7264), 607–613. https://doi.org/10.1038/nature08281

Su, T. (2022). Planetary boundary layer height (PBLH) over the SGP [Dataset]. *Zenodo*. https://doi.org/10.5281/zenodo.7374849

Su, T., Li, Z., & Kahn, R. (2020). A new method to retrieve the diurnal variability of planetary boundary layer height from LiDAR under different thermodynamic stability conditions. *Remote Sensing of Environment*, *237*, 111519. https://doi.org/10.1016/j.rse.2019.111519

Su, T., Li, Z., Roldan-Henao, N., Luan, Q., & Yu, F. (2024). Constraining effects of aerosol-cloud interaction by accounting for coupling between cloud and land surface. *Science Advances*, *10*(21), eadl5044. https://doi.org/10.1126/sciadv.adl5044

Su, T., Zheng, Y., & Li, Z. (2022). Methodology to determine the coupling of continental clouds with surface and boundary layer height under cloudy conditions from LiDAR and meteorological data. *Atmospheric Chemistry and Physics*, *22*(2), 1453–1466. https://doi.org/10.5194/acp-22-1453-2022

Tao, W. K., Chen, J. P., Li, Z., Wang, C., & Zhang, C. (2012). Impact of aerosols on convective clouds and precipitation. *Reviews of Geophysics*, *50*(2), 1–62. https://doi.org/10.1029/2011RG000369

Varble, A. (2018). Erroneous attribution of deep convective invigoration to aerosol concentration. *Journal of the Atmospheric Sciences*, *75*(4), 1351–1368. https://doi.org/10.1175/JAS-D-17-0217.1

Varble, A. C., Igel, A. L., Morrison, H., Grabowski, W. W., & Lebo, Z. J. (2023). Opinion: A critical evaluation of the evidence for aerosol invigoration of deep convection. *Atmospheric Chemistry and Physics*, *23*(21), 13791–13808. https://doi.org/10.5194/acp-23-13791-2023

Wang, D., Mace, G., & Turner, D. (n.d.-a). Merged sounding (MERGESONDE1MACE), 1996-07-15 to 2015-06-29, Southern Great Plains (SGP), central facility, Lamont, OK (C1) [Dataset]. *Atmospheric Radiation Measurement (ARM) User Facility*. https://doi.org/10.5439/1996752

Wang, D., Mace, G., & Turner, D. (n.d.-b). Merged sounding (MERGESONDE2MACE), 2002-01-01 to 2011-07-30, Southern Great Plains (SGP), central facility, Lamont, OK (C1) [Dataset]. *Atmospheric Radiation Measurement (ARM) User Facility*. https://doi.org/10.5439/1990004

Yuan, T., Remer, L. A., Pickering, K. E., & Yu, H. (2011). Observational evidence of aerosol enhancement of lightning activity and convective invigoration. *Geophysical Research Letters*, *38*(4), L04701. https://doi.org/10.1029/2010GL046052

Zhang, D., Shi, Y., & Riihimaki, L. (n.d.). Cloud type classification (CLDTYPE), 1996-11-08 to 2025-05-30, Southern Great Plains (SGP), central facility, Lamont, OK (C1) [Dataset]. *Atmospheric Radiation Measurement (ARM) User Facility*. https://doi.org/10.5439/1349884

Zhang, H., Su, T., Zheng, Y., & Li, Z. (2024). First assessment of cloud-land coupling in LASSO large-eddy simulations. *Geophysical Research Letters*, *51*(14), e2024GL109774. https://doi.org/10.1029/2024GL109774;REQUESTEDJOURNAL:JOURNAL:19448007;WGROUP:STRING:PUBLICATION

Zheng, Y., Rosenfeld, D., & Li, Z. (2018). Estimating the decoupling degree of subtropical marine stratocumulus decks from satellite. *Geophysical Research Letters*, *45*(22), 12560–12568. https://doi.org/10.1029/2018GL078382